

S' MoRE: Structural Mixture of Residual Experts for LLM Fine-tuning

Hanqing Zeng¹, Yinglong Xia¹, Zhuokai Zhao¹, Gilbert Jiang¹, Qiang Zhang¹, Jiayi Liu¹, Lizhu Zhang¹, Xiangjun Fan¹, Benyu Zhang¹

¹Meta AI

Fine-tuning pre-trained large language models (LLMs) presents a dual challenge of balancing parameter efficiency and model capacity. Existing methods like low-rank adaptations (LoRA) are efficient but lack flexibility, while Mixture-of-Experts (MoE) architectures enhance model capacity at the cost of more & under-utilized parameters. To address these limitations, we propose **Structural Mixture of Residual Experts** (👑 S' MoRE), a novel framework that seamlessly integrates the efficiency of LoRA with the flexibility of MoE. Specifically, S' MoRE employs *hierarchical* low-rank decomposition of expert weights, yielding residuals of varying orders *interconnected* in a multi-layer structure. By routing input tokens through sub-trees of residuals, S' MoRE emulates the capacity of many experts by instantiating and assembling just a few low-rank matrices. We craft the inter-layer propagation of S' MoRE's residuals as a special type of Graph Neural Network (GNN), and prove that under similar parameter budget, S' MoRE improves “structural flexibility” of traditional MoE (or Mixture-of-LoRA) by exponential order. Comprehensive theoretical analysis and empirical results demonstrate that S' MoRE achieves superior fine-tuning performance, offering a transformative approach for efficient LLM adaptation.

Date: April 10, 2025

Correspondence: First author at zengh@meta.com

Code: Coming soon



1 Introduction


Large language models (LLMs) have achieved remarkable success across a wide range of tasks by leveraging extensive pretraining on vast datasets, which equips them with general-purpose knowledge spanning diverse domains (Achiam et al., 2023; Dubey et al., 2024; Team et al., 2024; Liu et al., 2024a; Anthropic, 2024). However, the versatility of pre-trained LLMs often falls short when applied to specialized tasks or domains (Hadi et al., 2023; Ling et al., 2023; Chen et al., 2024) such as medical diagnostics (Tariq et al., 2024), legal reasoning (Yue et al., 2024), or personalized recommendation systems (Liu et al., 2024c), where domain-specific knowledge is critical. Fine-tuning addresses this limitation by adapting LLMs to specialized tasks, refining their capabilities to focus on the nuances of different domains (Zhang et al., 2023; Wang et al., 2024a, 2025). However, it introduces a fundamental tension between balancing parameter efficiency and the need for expanded model capacity to capture task-specific complexity (Wang et al., 2024b).

Existing approaches, such as Low-Rank Adaptations (LoRA) (Hu et al., 2021; Mao et al., 2025), have proven to be parameter efficient but often lack the flexibility required to adapt to complex tasks. On the other hand, Mixture-of-Experts (MoE) (Lepikhin et al., 2020; Fedus et al., 2022b; Cai et al., 2024; Dai et al., 2024) architectures provide the flexibility needed to handle such challenges. Compared to dense models, MoE improves model capacity by enabling conditional computation where different tokens activate different experts. However, traditional MoE approaches are often less parameter- or data-efficient since multiple experts need to learn their own parameters independently. In addition, when increasing the number of experts, there emerges a common challenge how to balance the experts' utilization while keeping the routing overhead low.

In addition to the total number of parameters, routing flexibility is another important factor in capacity scale-up. Recent studies (Dai et al., 2024; Ludziejewski et al., 2024; He, 2024) have empirically shown that under the same parameter budget, a large number of small (i.e., fine-grained) experts is more powerful than a small number of large experts. Ludziejewski et al. (2024) quantitatively summarized the MoE scaling law

with respect to experts’ granularity. DeepSeek-MoE (Dai et al., 2024) has provided an intuitive interpretation: Consider an MoE system with 16 rank-128 experts. Under top-2 routing, each token has $\binom{16}{2} = 120$ ways to select its own expert combination. If we break down each rank-128 expert as 4 rank-32 experts (and correspondingly use top-8 routing to keep the same activated parameters), each token now has $\binom{64}{8} = 4.4\text{G}$ routing choices.

Yet, is “breaking down experts into finer granularity” the most effective way of increasing routing flexibility? There are two potential limitations: 1. in PEFT fine-tuning, each expert already has a low rank, making it questionable whether finer granularity is desirable; 2. with more number of experts comes higher requirement on the router’s capability – it may be challenging to maintain good expert utilization when the number of experts grows. These motivate us to take a different approach. To emulate more routing choices *without* increasing the number of experts, we exploit the *power of structure*. We arrange experts into multiple layers, and the router customizes a sub-tree for each token (instead of just determining the indices of the active experts). The key point is that *the same set of experts can form many different (non-isomorphic) sub-trees* when the experts connect to each other differently. We correspondingly extend the concept of routing flexibility into **structural flexibility**, and theoretically quantify the exponential growth of structural flexibility for S’MoRE.

Proposed work. We propose **Structural Mixture of Residual Experts** ( S’MoRE), a novel PEFT architecture that improves MoE’s model flexibility & capacity by exploiting experts’ structural relationship, while being as parameter-efficient as LoRA. To build S’MoRE, we start from the idea of hierarchical residual decomposition of expert weights, where low-rank parameters of different orders form a multi-layer inter-connection network. We craft the model architecture so that when residuals aggregate and propagate across layers, they 1. remain low-rank to maintain overall efficiency, 2. can generate distinct embeddings for *all* non-isomorphic router-selected sub-trees, which theoretically guarantees high structural flexibility, and 3. are able to express the standard single-layer MoE model variants, which makes S’MoRE a strictly more powerful upgrade. To customize the expert structure for each token, we design a hierarchical router that efficiently and iteratively selects the children residuals when traversing down the selected ancestors. S’MoRE can be conceptually seen as a novel Graph Neural Network (GNN), where the “graph” emerges dynamically from the router’s selection, and each S’MoRE layer simulates a color-refinement step in the classic graph isomorphism test (Huang and Villar, 2021; Xu et al., 2019). Overall, S’MoRE achieves the benefits of both LoRA and fine-grained MoE, and addresses their limitations by exploiting experts’ structure – S’MoRE emulates the capacity of *exponentially more* experts than physically instantiated, while keeping each residual low-rank. We extensively evaluate S’MoRE on 2 base models (LLaMA 3.2 1B, LLaMA 3 8B), 5 fine-tuning benchmarks (reasoning and other domain-specific tasks), 3 router gate architectures (dense and sparse), and across different scales (2-layer and 3-layer). S’MoRE consistently and significantly outperform state-of-the-art models and 1-layer baselines in terms of both accuracy (2.1% higher) and parameter efficiency (16% less), indicating that structural flexibility may be a critical factor in model capacity scaling-up for fine-tuning tasks and beyond.

2 Related Work

Parameter efficient fine-tuning (PEFT). Given a large pre-trained model, PEFT learns a light-weight adapter whose number of trainable parameters is just a small fraction of that of the pre-trained model, to efficiently adapt to various downstream tasks. LoRA (Hu et al., 2021) and the many variants (Liu et al., 2024b; Kopiczko et al., 2024) have gained much popularity, due to their simplicity and good empirical performance. The main idea is to learn a low-rank matrix on top of each full-rank pre-trained matrix, where the rank controls the efficiency-accuracy tradeoff. However, despite the high parameter efficiency, these methods may be bottlenecked by their limited model capacity since the adapter is just learning the same linear projection for all input tokens.

Mixture-of-Experts (MoE). Mixture-of-Experts designs have been shown to boost LLM’s model capacity (Dai et al., 2024; Fedus et al., 2022b; Puigcerver et al., 2024) due to their flexibility in conditionally activate different set of parameters for different input tokens. Recent works have developed MoE variants in the context of PEFT. MixLoRA (Li et al., 2024) constructs the adapter as a series of LoRA experts where each token selects its own top- k experts to activate. Similarly, MoLE (Wu et al., 2024) considers a flat layer of

LoRA experts and enhances the expert composition via a learnable gate implementing flexible branch selection. MoV and MoLORA (Zadouri et al., 2024) proposes a MoE variant that mixes (IA)³ vectors (Liu et al., 2022) or LoRA weights for adapting attention modules during fine-tuning. HydraLoRA (Tian et al., 2024) splits each up-projection \mathbf{B} matrix of LoRA into multiple heads, and then performs weighted sum of each head’s output where the weights are customized for each token by a dense gate. For the above PEFT-MoE models, the gating module for selecting experts are often based on classic designs of sparse or dense gates, such as the noisy top- k gate (Shazeer et al., 2017) or the switch-transformer gate (Fedus et al., 2022b). Thus, if we blindly increase the number of experts in PEFT, it becomes a challenge how to ensure that all experts are well utilized (Fedus et al., 2022a). Such limitation to model scale-up can be addressed by experts’ structural composition in S’MoRE. In addition, there is an emerging trend to research the unique scaling behaviors of MoE systems compared with dense models. Ludziejewski et al. (2024) summarizes a scaling law which indicates that finer expert granularity may benefit model capacity, and He (2024) provides a practical implementation where the number of experts becomes very large. Through our analysis and experiments, we hypothesize that “structural flexibility” may be a neglected yet critical factor determining MoE scaling. Thus, S’MoRE has the potential to scale better than the current MoE models, for fine-tuning tasks or beyond.

Heterogeneous experts. In most MoE models, experts are homogeneous and may have an identical model architecture. Heterogeneous experts have been recently explored in language modeling (Raposo et al., 2024; Ainslie et al., 2023) and graph learning (Zeng et al., 2024). MoD (Raposo et al., 2024) and CoLT5 (Ainslie et al., 2023) consider the combination of light and heavy experts so that tokens through the light path can be processed faster and more cheaply. Mowst (Zeng et al., 2024) further discovers that mixture of weak and strong experts can enhance the MoE’s capacity beyond that of a strong expert alone. However, existing heterogeneous MoE designs consider a “horizontal” stacking of different types of experts, where the weak/light branch operates in parallel to the strong/heavy one. In S’MoRE, the residuals of different orders can also be interpreted as experts of different strength (with the 1st-order residuals being the strongest). Yet, we explore a “vertical” stacking design where the higher-order residuals transform and propagate to the lower-order ones. The heterogeneous expert design in S’MoRE encodes additional structural information than existing models.

3 Preliminaries

We first introduce the preliminaries of two mainstream fine-tuning techniques. We consider one transformer layer and omit the layer index. Let $\mathbf{x} \in \mathbb{R}^d$ denote the d -dimensional token embedding vector.

LoRA formulation. The adapter consists of a down-projection matrix $\mathbf{A} \in \mathbb{R}^{d \times r}$ and an up-projection matrix $\mathbf{B} \in \mathbb{R}^{r \times d}$, where the rank $r \ll d$ to achieve parameter efficiency. LoRA performs the following to map input token embedding \mathbf{x} to adapter’s output \mathbf{x}' :

$$\mathbf{x}' = \mathbf{B} \cdot \mathbf{A} \cdot \mathbf{x} \quad (1)$$

MoE formulation. Let s be the number of experts. The routing function $\text{ROUTE}(\cdot)$ maps each input token to the corresponding experts, where $\text{ROUTE}(\mathbf{x})^i \in \mathbb{R}$ gives expert i ’s score for token \mathbf{x} . Suppose each expert i performs a linear transformation of \mathbf{x} via matrix \mathbf{W}^i . The MoE layer performs:

$$\mathbf{x}' = \sum_{i=1}^s \text{ROUTE}(\mathbf{x})^i \cdot \mathbf{W}^i \cdot \mathbf{x} \quad (2)$$

If the router performs top- k sparse gating, then only k values of $\text{ROUTE}(\mathbf{x})^i$ are non-zero. All the s scores, $\text{ROUTE}(\mathbf{x})^i$, may optionally be normalized (e.g., by softmax).

Remark. All adapters discussed here can be applied to both the FFN and self-attention modules of a transformer layer. The adapter output \mathbf{x}' is added back to the output generated by the pre-trained weight.

4 S'MoRE

4.1 Low-Rank MoE Variants

Mixture of low-rank experts (MoLRE). Various works (Wu et al., 2024; Dou et al., 2024; Li et al., 2024) have combined LoRA and MoE to mix low-rank experts. Specifically, they replace the full-rank matrix \mathbf{W}^i in Eq. (2) with a low-rank one $\mathbf{B}^i \cdot \mathbf{A}^i$. In this paper, we term such model as *mixture of low-rank experts (MoLRE)*.

Mixture of multi-order residues (MoMOR). In fact, we can view $\mathbf{B}^i \cdot \mathbf{A}^i$ as an 1st-order approximation of the original \mathbf{W}^i . Following this idea, we apply such approximation iteratively as $\mathbf{W}^i \approx \sum_{\ell=0}^{L-1} \Delta \mathbf{W}_\ell^i$, where $\Delta \mathbf{W}_\ell^i$ is the $(\ell + 1)$ th-order residue term (and thus, $\Delta \mathbf{W}_0^i = \mathbf{B}^i \cdot \mathbf{A}^i$). Each $\Delta \mathbf{W}_\ell^i$ can still maintain a low rank r_ℓ , as the sum of these low rank matrices can have a higher rank. Specifically, $\sum_{\ell=0}^{L-1} \Delta \mathbf{W}_\ell^i$ can have rank up to $\sum_{\ell=0}^{L-1} r_\ell$.

Building upon this, we introduce an extension of MoLRE, which we call *mixture of multi-order residues (MoMOR)*. Specifically, let $\mathcal{R}_\ell = \{\Delta \mathbf{W}_\ell^1, \Delta \mathbf{W}_\ell^2, \dots\}$ be the set of order- $(\ell + 1)$ residues, MoMOR model performs the following for orders 1 to L :

$$\mathbf{x}' = \sum_{\ell=0}^{L-1} \sum_{i=1}^{s_\ell} \text{ROUTE}_\ell(\mathbf{x})^i \cdot \Delta \mathbf{W}_\ell^i \cdot \mathbf{x} \quad (3)$$

where the model dynamically selects and combines different orders of residuals using a routing mechanism. Each $\text{ROUTE}_\ell(\mathbf{x})^i$ serves as a gating function that determines the contribution of the corresponding residue $\Delta \mathbf{W}_\ell^i$, allowing the model to flexibly mix and match multi-order approximations in a data-dependent manner. By leveraging this mixture-of-experts-style routing, MoMOR can adaptively distribute computation across different levels of approximation, improving both efficiency and expressivity.

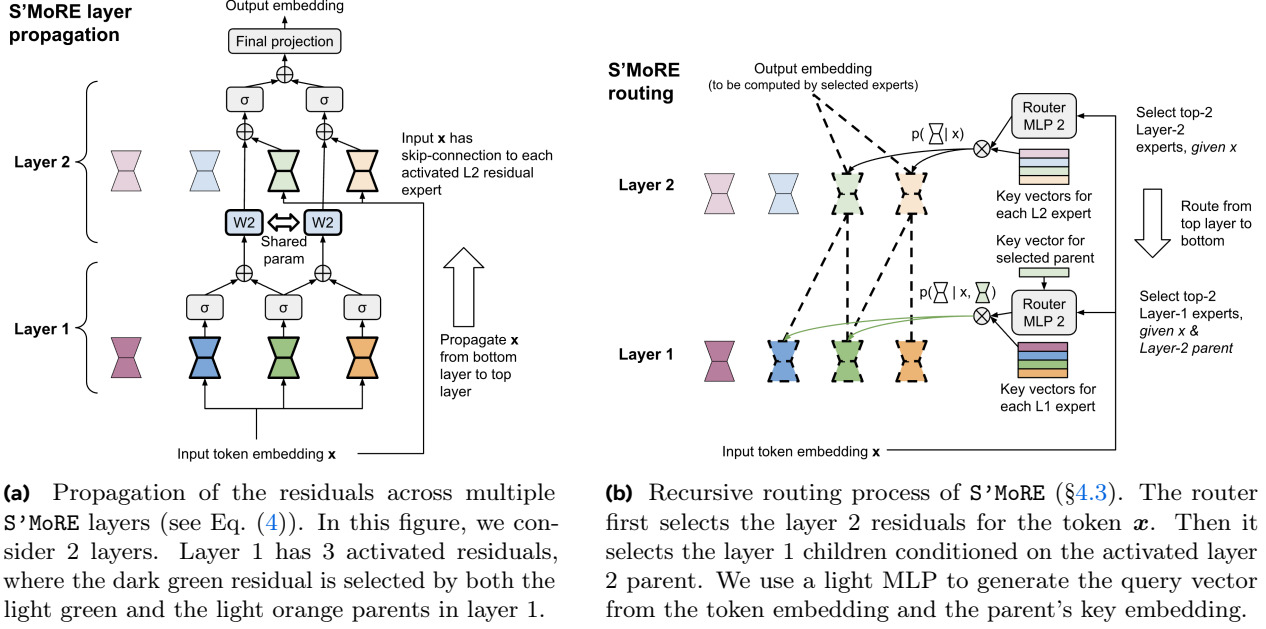
Notably, when $L = 2$ and $s_\ell = 1$, Eq. (3) simplifies to $\mathbf{x}' = \Delta \mathbf{W}_0^1 \cdot \mathbf{x} + \sum_{i=1}^{s_2} \text{ROUTE}_1(\mathbf{x})^i \cdot \Delta \mathbf{W}_1^i \cdot \mathbf{x}$, where MoMOR reduces to a special MoE with a *shared* expert – a design choice seen in models such as DeepSeek-v3 (DeepSeek-AI, 2024) and many others (Rajbhandari et al., 2022; Li et al., 2024).

4.2 Structural Mixture

We now derive S'MoRE. We consider applying S'MoRE to each transformer layer. In the following, “layer” refers to a S'MoRE layer with a collection of residual experts (rather than a transformer layer). Based on MoMOR, we arrange all the residues $\mathcal{R}_0, \dots, \mathcal{R}_{L-1}$ into a L -layer structure. When a token \mathbf{x} comes, we activate a sub-structure that interconnects correlated residues in adjacent layers. The token propagates along the sub-structure layer by layer, where each layer implements a lightweight function to aggregate previous-layer residues. Extending the standard MoE to multiple layers improves model capacity by drastically increasing the model’s “structural flexibility” (see §4.5).

Parameters. Let $\mathbf{x} \in \mathbb{R}^d$ be the d -dimensional token embedding. Layer $\ell + 1$ (for $0 \leq \ell \leq L - 1$) consists of s_ℓ residual experts. Each expert i (for $1 \leq i \leq s_\ell$) is instantiated by a down-projection matrix $\mathbf{A}_\ell^i \in \mathbb{R}^{r_\ell \times d}$ and an up-projection matrix $\mathbf{B}_\ell^i \in \mathbb{R}^{d_{\ell+1} \times r_\ell}$, where r_ℓ is the experts’ rank and $d_{\ell+1}$ is the output dimension of layer $\ell + 1$. Layer $\ell + 1$ also has a learnable matrix $\mathbf{W}_\ell \in \mathbb{R}^{d_{\ell+1} \times d_\ell}$ that projects the layer- ℓ output embedding to the $d_{\ell+1}$ -dimensional sub-space. Thus, \mathcal{R}_ℓ consists of all \mathbf{A}_ℓ^i and \mathbf{B}_ℓ^i for $1 \leq i \leq s_\ell$.

Propagation. Each token \mathbf{x} propagates in the L -layer structure in two phases. In the *routing* phase, the router activates the best-matching experts in a top-down manner, from layer L down to layer 1. For the final layer L , the router selects from \mathcal{R}_{L-1} based on standard sparse gating modules (e.g., Shazeer et al. (2017)). For an intermediate layer $\ell < L$, the router computes the probability to activate an expert in $\mathcal{R}_{\ell-1}$, *conditioned* on the already activated ancestor experts in layers $\ell' > \ell$. This conditional selection process ensures that the activated experts in adjacent layers are connected. Different from the router of traditional MoE models, the S'MoRE router customizes a depth- L “residual tree” for each input token. We discuss the



(a) Propagation of the residuals across multiple S'MoRE layers (see Eq. (4)). In this figure, we consider 2 layers. Layer 1 has 3 activated residuals, where the dark green residual is selected by both the light green and the light orange parents in layer 1.

(b) Recursive routing process of S'MoRE (§4.3). The router first selects the layer 2 residuals for the token x . Then it selects the layer 1 children conditioned on the activated layer 2 parent. We use a light MLP to generate the query vector from the token embedding and the parent's key embedding.

Figure 1 Illustration of the layer propagation and routing process of S'MoRE.

more detailed router architecture in §4.3 and analyze the boosted structural flexibility due to the tree-based routing in §4.5.

In the *aggregation phase*, the token propagates along the activated residual tree in a bottom-up manner, from layer 1 up to L . Layer $\ell + 1$ aggregates the information from the activated children experts in \mathcal{R}_ℓ , and generates output embedding for the parent expert in $\mathcal{R}_{\ell+1}$. For each parent expert i , define \mathcal{N}_ℓ^i as the set containing the indices of i 's children. Layer $\ell + 1$ operates as follows:

$$\mathbf{x}_{\ell+1}^i = \sum_{n \in \mathcal{N}_\ell^i} \alpha_\ell^{i,n} \cdot \sigma(\mathbf{B}_\ell^n \cdot \mathbf{A}_\ell^n \cdot \mathbf{x} + \mathbf{W}_\ell \cdot \mathbf{x}_\ell^n) \quad (4)$$

where $\sigma(\cdot)$ is a non-linear function which can be just an activation function (e.g., ReLU (Agarap, 2018)) or a lightweight MLP. The scalar coefficient $\alpha_\ell^{i,n}$ is the score generated by the router, which will be further elaborated in §4.3. Inputs to Eq. (4) consists of two parts:

- Raw token embedding \mathbf{x} , which functions as skip connection for different-order residues $\mathbf{B}_\ell^n \cdot \mathbf{A}_\ell^n$.
- Embedding \mathbf{x}_ℓ^n output from the previous layer, which enables *deep* interaction among different-order residues given non-linear $\sigma(\cdot)$ (in comparison to the shallow aggregation in Eq. (3)).

Note that for the first layer ($\ell = 0$), input \mathbf{x}_0^n does not exist. To ease notation, we manually define \mathbf{x}_0^i as an empty vector in \mathbb{R}^0 with $d_0 := 0$. This gives an empty matrix $\mathbf{W}_0 \in \mathbb{R}^{d_1 \times 0}$, and Eq. (4) applies to all layers $0 \leq \ell \leq L - 1$. For the last layer L , we have a single output node ($s_L = 1$) that is generated by aggregating information from all the multi-order residues. So we define $\mathbf{x}_L := \mathbf{x}_L^0$.

Dimensionality d_ℓ . We discuss how to set the output embedding dimensionality d_ℓ for layer ℓ in order to 1. avoid information loss in the aggregation process, and 2. keep the overall L -layer propagation efficient. If we borrow the design from LoRA, a simple choice would be $d_{\ell+1} = d$, where d can be orders of magnitude larger than r_ℓ (e.g., 4096 for LLaMA models (Dubey et al., 2024)). However, such a large $d_{\ell+1}$ makes the subsequent multiplication with \mathbf{W}_ℓ prohibitively expensive.

To reduce the computation cost, our objective is to find the smallest $d_{\ell+1}$ such that it does not incur any information loss compared to the vanilla setting of $d_{\ell+1} = d$. The problem is equivalent to finding the maximum dimension of the subspace that $\mathbf{x}_{\ell+1}^i$ can possibly span following Eq. (4), for any choices of \mathcal{N}_ℓ^i , \mathbf{B}_ℓ^n , \mathbf{A}_ℓ^n and any i that may be activated.

To simplify discussion, we ignore activation $\sigma(\cdot)$. Notice that: 1. For a given n and any \mathbf{x} , the output $\mathbf{B}_\ell^n \cdot \mathbf{A}_\ell^n \cdot \mathbf{x}$ maximally spans a d' -dimensional subspace of the original \mathbb{R}^d . Such subspace is defined by the projection matrix $\mathbf{B}_\ell^n \cdot \mathbf{A}_\ell^n$ with max rank $d' = \min\{d_{\ell+1}, r_\ell\}$; 2. There are s_ℓ possible choices of n , leading to s_ℓ different d' -dimensional subspace. When all such subspaces are orthogonal to each other, they jointly form a d'' -dimensional subspace where $d'' = \min\{d_{\ell+1}, s_\ell \cdot r_\ell\}$; 3. $\mathbf{W}_\ell \cdot \mathbf{x}_\ell^n$ can span another subspace of dimension $\min\{d_{\ell+1}, d_\ell\}$ defined by \mathbf{W}_ℓ (independent of n). For all n , the term $\mathbf{B}_\ell^n \cdot \mathbf{A}_\ell^n \cdot \mathbf{x} + \mathbf{W}_\ell \cdot \mathbf{x}_\ell^n$ maximally spans a d''' -dimensional subspace, with $d''' = \min\{d_{\ell+1}, d_\ell + s_\ell \cdot r_\ell\}$; and 4. Since a subspace is closed under linear combinations, the aggregation $\sum_{n \in \mathcal{N}_\ell^i} \alpha_\ell^{i,n} (\mathbf{B}_\ell^n \cdot \mathbf{A}_\ell^n \cdot \mathbf{x} + \mathbf{W}_\ell \cdot \mathbf{x}_\ell^n)$ remains in the d''' -dimensional subspace, regardless of \mathcal{N}_ℓ^i .

For the vanilla case of $d_{\ell+1} = d$, assuming d is large enough, we have $d''' = d_\ell + s_\ell \cdot r_\ell$. Thus, to avoid information loss, we need to preserve such a d''' . The minimum $d_{\ell+1}$ satisfying this should follow the recursion:

$$d_{\ell+1} = d_\ell + s_\ell \cdot r_\ell, \quad \text{where } d_0 := 0 \text{ and } \ell \in [0, L-1] \quad (5)$$

which generalizes to:

$$d_\ell = \sum_{i=0}^{\ell-1} s_i \cdot r_i \quad (6)$$

Final projection. After the last layer L , we need an additional linear projection to map the d_L -dimensional output \mathbf{x}_L to the final output dimension d_{out} (i.e., d_{out} is the dimensionality of \mathbf{x}' in Equations 2 and 3). We thus need a projection matrix $\mathbf{W}_{\text{proj}} \in \mathbb{R}^{d_L \times d}$ that simply performs:

$$\mathbf{x}' = \mathbf{W}_{\text{proj}} \cdot \mathbf{x}_L \quad (7)$$

4.3 Hierarchical Routing

As discussed in §4.2, the router selects the experts to activate in a top-down manner. We start from the last layer L . The router computes $p(i_{L-1} | \mathbf{x})$, which is the probability to activate an expert i_{L-1} in \mathcal{R}_{L-1} given token \mathbf{x} . The top- f_{L-1} experts with the highest $p(i_{L-1} | \mathbf{x})$ are selected. Next, for each selected expert i_{L-1} , we compute $p(i_{L-2} | i_{L-1}, \mathbf{x})$, which is the conditional probability to activate an expert i_{L-2} in \mathcal{R}_{L-2} given its activated parent i_{L-1} and input \mathbf{x} . Each activated expert i_{L-1} further activates f_{L-2} children experts with the highest $p(i_{L-2} | i_{L-1}, \mathbf{x})$. In general, on layer ℓ , the router computes the conditional probability $p(i_{\ell-1} | i_{L-1}, \dots, i_\ell, \mathbf{x})$, with i_{L-1}, \dots, i_ℓ being all the activated ancestors of the candidate expert $i_{\ell-1}$. The activated experts of all layers form a depth- L tree. Each depth- ℓ node fans out to $f_{L-\ell}$ children experts (the activated layer- L experts are the depth-1 nodes in the tree).

As above, let f_ℓ be the fanout factor of each parent expert, F_ℓ be the total number of experts selected from \mathcal{R}_ℓ (i.e., F_ℓ is the total number of depth- $(L-\ell)$ experts in the activated tree), F_ℓ is calculated as:

$$F_\ell = \prod_{i=\ell}^{L-1} f_i \quad (8)$$

Note that the same expert in \mathcal{R}_ℓ can be selected multiple times by different paths of ancestors. It is possible that $F_\ell > s_\ell$ where s_ℓ is total number of distinct experts in \mathcal{R}_ℓ .

The router computes the similarity among the token \mathbf{x} , the ancestor experts and the candidate expert to generate conditional probability $p(i_\ell | i_{L-1}, \dots, i_{\ell+1}, \mathbf{x})$. We use dot product to measure similarity. Specifically, for each expert i in \mathcal{R}_ℓ , we instantiate a learnable m -dimensional *key* vector \mathbf{k}_ℓ^i . For the whole candidate pool \mathcal{R}_ℓ , we instantiate a neural network, $\text{MLP}_\ell(\cdot)$, to generate an m -dimensional *query* vector based on \mathbf{x} and the ancestor experts. The routing probability over \mathcal{R}_ℓ is computed by the normalized key-query dot product.

For a path of activated ancestors, “expert i' in $\mathcal{R}_{\ell+1}$, ..., expert i''' in \mathcal{R}_{L-1} ”, the router generates the query vector \mathbf{q} and the router score α_ℓ^i as follows:

$$\begin{aligned} \mathbf{q} &= \text{MLP}_\ell \left(\text{concat} \left(\mathbf{x}, \mathbf{k}_{\ell+1}^{i'}, \dots, \mathbf{k}_{L-1}^{i'''} \right) \right) \\ \alpha_\ell^i &= \text{softmax}(\mathbf{k}_\ell^i \cdot \mathbf{q}) \end{aligned} \quad (9)$$

where $\text{concat}(\cdot)$ performs vector concatenation and $\text{softmax}(\cdot)$ normalizes over \mathcal{R}_ℓ .

Computation optimization. Eq. (9) can be computationally expensive when all $\text{MLP}_\ell(\cdot)$ need to process the high-dimensional \mathbf{x} (e.g., \mathbf{x} has 4096 dimensions for LLaMA (Dubey et al., 2024)). To reduce computation cost, we first project the d -dimensional \mathbf{x} to a d_{down} -dimensional \mathbf{x}_{down} (e.g., $d_{\text{down}} = 32$), and then replace \mathbf{x} with \mathbf{x}_{down} in Eq. (9). The dimension of the input to $\text{MLP}_\ell(\cdot)$ then becomes $d_{\text{down}} + (L - \ell - 1) \cdot m$.

Gating types. The router and layer propagation designs described above are compatible to various types of gates, including sparse gates as well as dense ones. In our experiments (§5), we have implemented and evaluated 3 types of gates:

- Sparse noisy top- k (Shazeer et al., 2017): For each layer ℓ , the router selects the top $k = f_\ell$ children residuals with the highest gating scores (generated by Eq. (9)). However, a common issue with sparse expert selection is expert under-utilization, where certain experts are overused while others remain idle, resulting in inefficient training dynamics. To address this, following (Shazeer et al., 2017), we first add a learnable noise term on top of gating score α , to encourage exploration. Then we implement a layer-wise importance loss plus balance loss, computed separately for each set of experts \mathcal{R}_ℓ based on gating score distribution and activation frequency. We sum up the importance loss of each S'MoRE layer and each transformer layer, and add it to the model prediction cross-entropy (CE) loss, i.e.,

$$\mathcal{L}_{\text{total}} = \mathcal{L}_{\text{CE}} + \gamma \cdot \sum_{\ell_{\text{trans}}=1}^{L_{\text{trans}}} \sum_{\ell=1}^L \left(\mathcal{L}_{\ell_{\text{trans}}, \ell}^{\text{importance}} + \mathcal{L}_{\ell_{\text{trans}}, \ell}^{\text{balance}} \right), \quad (10)$$

where L_{trans} denotes the total number of transformer layers and γ is a coefficient ($\ll 1$) controlling the strength of the load-balance constraint.

- Sparse switch-transformer (Fedus et al., 2022b): This is another popular sparse gate design. There are two main differences from the noisy top- k gate above. First, the switch gate implements an optional jitter noise that is applied to the gate's input embedding rather than the final gating score. In addition, the switch gate integrates a different way to compute the load-balance auxiliary loss. The auxiliary loss is still added back to the CE loss of the main task.
- Dense: Here we activate all children experts, meaning that $f_\ell = s_\ell$. For each children, the expert score α is still generated by the gating neural net. So the dense gate can be understood as a soft version of the sparse gates above. Now since all experts are activated, we do not include additional auxiliary loss for load-balance. The dense gate is used by HydraLoRA (Tian et al., 2024) which we include as one of the experimental baselines (§5).

4.4 Parameter & Computation Efficiency

Although S'MoRE introduces more layers than traditional MoE designs, the overall model remains efficient in terms of both trainable parameters and computation – **S'MoRE is as efficient as the vanilla LoRA under the same total rank**. Our following analysis is based on the layer propagation Eq. (4) and the gating function Eq. (9).

Parameter efficiency. Each S'MoRE layer $\ell + 1$ consists of the following trainable parameters: \mathbf{B}_ℓ^n , \mathbf{A}_ℓ^n and \mathbf{W}_ℓ . The total trainable parameters equals:

$$\begin{aligned} P_{\ell+1} &= s_\ell \cdot (d \cdot r_\ell + r_\ell \cdot d_{\ell+1}) + d_\ell \cdot d_{\ell+1} \\ &= s_\ell \cdot d \cdot r_\ell + d_{\ell+1} \cdot (s_\ell \cdot r_\ell + d_\ell) \\ &\stackrel{(a)}{=} s_\ell \cdot d \cdot r_\ell + d_{\ell+1}^2 \end{aligned} \quad (11)$$

where the last step “(a)” is according to Eq. (5). The final projection matrix according to Eq. (7) requires $P_{\text{proj}} = d \cdot d_L$ parameters. So the total number of parameters for all S'MoRE layers equals:

$$\begin{aligned}
P_{\text{proj}} + \sum_{\ell=1}^L P_{\ell} &= d \cdot d_L + d \cdot \left(\sum_{\ell=0}^{L-1} s_{\ell} \cdot r_{\ell} \right) + \Delta \\
&\stackrel{(b)}{=} 2 \cdot d \cdot d_L + \Delta \\
&\stackrel{(c)}{\approx} 2 \cdot d \cdot d_L
\end{aligned} \tag{12}$$

$$\text{where } \Delta = \sum_{\ell=1}^L d_{\ell}^2$$

Note that step “(b)” above is according to Eq. (6); Δ is the parameter overhead in order to support multi-layer propagation. In PEFT, we have $d_1 < \dots < d_L \ll d$ (e.g., d_L may be 64, while $d = 4096$ or even larger). Therefore, $\Delta \ll 2 \cdot d \cdot d_L$, and this leads to step “(c)” above.

For the router, the trainable parameters consist of two parts. The first part is to down-project input token \mathbf{x} to \mathbf{x}_{down} , which contributes to $d \cdot d_{\text{down}}$ parameters. The second part is the MLP per layer. As discussed in §4.3, the dimension of the input to the MLP is $d_{\text{down}} + (L - \ell) \cdot m$ for layers $\ell = 1, \dots, L$, where $m \ll d$ is the dimension of the key vectors. In our experiments, we set the hidden dimension of the MLPs simply as m . Since m and d_{down} are both very small, the overall parameter count for the routers is small in practice.

In conclusion, the total trainable parameters for all S²MoRE layers is approximately $2 \cdot d \cdot d_L$, which is **the same as the parameter count for a vanilla LoRA with rank d_L** (the 2 factor corresponds to the down-projection \mathbf{A} and up-project \mathbf{B} matrices).

Computation cost. In Eq. (4), each $\mathbf{B}_{\ell}^n \cdot \mathbf{A}_{\ell}^n \cdot \mathbf{x}$ term requires $C' = d \cdot r_{\ell} + r_{\ell} \cdot d_{\ell+1}$ operations. Each $\mathbf{W}_{\ell} \cdot \mathbf{x}_{\ell}^n$ requires $C'' = d_{\ell} \cdot d_{\ell+1}$ operations. Consider all activated experts i in layer $\ell + 1$, there can be at most $N' = \min\{s_{\ell}, F_{\ell}\}$ distinct $\mathbf{B}_{\ell}^n \cdot \mathbf{A}_{\ell}^n$ terms, meaning that the C' cost is only incurred N' times. There are F_{ℓ} number of different \mathbf{x}_{ℓ}^n inputs, each incurring C_2 cost. Ignoring the cost of addition “ $\sum_{n \in \mathcal{N}_{\ell}^i}$ ” and scalar multiplication by $\alpha_{\ell}^{i,n}$, the total cost of layer $\ell + 1$ equals:

$$\begin{aligned}
C_{\ell+1} &\leq \min\{s_{\ell}, F_{\ell}\} \cdot r_{\ell} \cdot (d + d_{\ell+1}) + F_{\ell} \cdot d_{\ell} \cdot d_{\ell+1} \\
&\leq s_{\ell} \cdot r_{\ell} \cdot d + F_{\ell} \cdot d_{\ell+1} \cdot (d_{\ell} + r_{\ell})
\end{aligned} \tag{13}$$

where d_{ℓ} and F_{ℓ} follow Eq. (6) and Eq. (8).

The cost of the final projection (Eq. (7)) equals $C_{\text{proj}} = d \cdot d_L$. So the total computation cost is:

$$\begin{aligned}
C_{\text{proj}} + \sum_{\ell=1}^L C_{\ell} &= d \cdot d_L + d \cdot \left(\sum_{\ell=0}^{L-1} s_{\ell} \cdot r_{\ell} \right) + \Delta' \\
&\stackrel{(b)}{=} 2 \cdot d \cdot d_L + \Delta' \\
&\stackrel{(c)}{\approx} 2 \cdot d \cdot d_L
\end{aligned} \tag{14}$$

$$\text{where } \Delta' \leq \sum_{\ell=0}^{L-1} F_{\ell} \cdot d_{\ell+1} \cdot (d_{\ell} + r_{\ell})$$

where steps “(b)” and “(c)” follow similar reasoning to Eq. (12).

Particularly, under practical values of $d_{\ell} + r_{\ell} \leq d_{\ell+1} \ll d$, the overhead term Δ' is small or negligible compared to the main cost $2 \cdot d \cdot d_L$. To empirically verify the approximation, in Table 1, we calculate the value of $2 \cdot d \cdot d_L$, the overhead Δ' , and their ratio. We take a representative configuration with $f_{\ell} = 2$, $s_{\ell} = 4$, and $r_{\ell} = 8$ or 16 for all layers ℓ (consistent with our experiments in §5).

We increase the total number of layers L from 2 to 4. In practice, the overhead Δ' is indeed small. For 2 layers, the overhead is just **1.2%** (or **2.3%**) of the cost of vanilla LoRA with rank $d_L = 64$ (or $d_L = 128$).

The cost of the gating MLPs can be derived in a similar fashion as above (see the ‘‘Parameter efficiency’’ paragraph). The conclusion is that the gating MLPs are lightweight compared to the main cost $2 \cdot d \cdot d_L$, due to the small input, output and hidden dimensions of the MLPs.

In conclusion, the total computation cost of S'MoRE is approximately $2 \cdot d \cdot d_L$, which is **the same as the cost of a vanilla LoRA with rank d_L** . So far, we have validated both the parameter and the computation efficiency of S'MoRE, compared with vanilla LoRA. We next analyze how S'MoRE improves the model capacity.

Table 1 Overhead Δ' compared with the main computation cost $2 \cdot d \cdot d_L$

r_ℓ	L	d_L	$2 \cdot d \cdot d_L$	Δ'	Overhead ratio
8	2	64	0.5M	0.006M	1.2%
	3	96	0.8M	0.026M	3.3%
	4	128	1.0M	0.079M	7.5%
16	2	128	1.0M	0.025M	2.3%
	3	192	1.6M	0.104M	6.6%
	4	256	2.1M	0.315M	15.0%

4.5 Model Capacity

In this section, we theoretically justify how S'MoRE enhances model capacity compared with baseline models. First, we show that the two low-rank MoE variants in §4.1 (MoLRE and MoMOR) are strictly special cases of S'MoRE.

Proposition 4.1. *S'MoRE can express MoLRE, when $L = 1$.*

Proposition 4.2. *S'MoRE can express MoMOR, when setting $\sigma(\cdot)$ as the identity mapping.*

The above two propositions say that, for any MoLRE (or MoMOR) model, we can find a corresponding S'MoRE model that generates identical output as MoLRE (or MoMOR) for any input \mathbf{x} . The proof of Proposition 4.1 is obvious: when $L = 1$, Eq. (4) reduces to Eq. (2). For Proposition 4.2, when we remove σ , we can collapse a multi-layer network into a single layer equivalent. In addition, we need to set the dimensionality according to Eq. (6) to avoid information loss compared to MoMOR. It is thus easy to show that the multi-layer S'MoRE with identity mapping σ exactly reduces to Eq. (3).

Can S'MoRE be theoretically better than MoLRE and MoMOR, if we go beyond the constraints of Propositions 4.1 and 4.2 by setting $L > 1$ and σ as non-linear mapping? To answer it, we analyze an MoE model’s expressive power by quantifying the **structural flexibility**.

Structural flexibility. Let Θ be the collection of all experts’ parameters including \mathbf{B}_ℓ^i , \mathbf{A}_ℓ^i and \mathbf{W}_ℓ for $0 \leq \ell \leq L - 1$ and all valid i . Given Θ , when a token \mathbf{x} comes, different routers may activate different residue experts, and thus generate different output embedding \mathbf{x}_L . Therefore, we define $\text{dist}(\mathbf{x}; \Theta)$ as the number of *distinct* \mathbf{x}_L . The larger $\text{dist}(\mathbf{x}; \Theta)$ can be, the more ‘‘structurally flexible’’ the model architecture is. Note that our focus here is on the multi-layer structure formed by the residual experts, rather than the router network (thus, we assume an ideal router for the following Theorems).

Next, we show that including non-linearity σ in S'MoRE makes the model significantly more structurally flexible, which justifies S'MoRE’s higher model capacity than MoMOR. In the next Theorems, we ignore the α_ℓ^n scalar factor when generating \mathbf{x}_L .

Theorem 4.3. *The structural flexibility of MoMOR is upper bound by $\Gamma_{\text{MoMOR}} = \max_{\mathbf{x}, \Theta} \text{dist}(\mathbf{x}; \Theta) \leq \binom{s_{L-1}}{f_{L-1}} \cdot \prod_{\ell=0}^{L-2} \left(\sum_{i=f_\ell}^{\min\{F_\ell, s_\ell\}} \binom{s_\ell}{i} \right)$.*

Theorem 4.4. *When implementing $\sigma(\cdot)$ as an MLP, there exists some Θ' such that the structural flexibility of S'MoRE is lower bound by $\Gamma_{\text{S'MoRE}} = \min_{\mathbf{x}} \text{dist}(\mathbf{x}; \Theta') = \prod_{\ell=0}^{L-1} \binom{s_\ell}{f_\ell}^{F_{\ell+1}}$, where we define $F_L = 1$.*

In Theorems 4.3 and 4.4, $\binom{s}{k} = \frac{s!}{k!(s-k)!}$ is the binomial coefficient quantifying the total number of ways to choose k items from a set of s items without considering order. And F_ℓ is defined in Eq. (8). Note that Theorem 4.3 gives the upper bound while Theorem 4.4 shows the lower bound. However, when increasing the number of layers, the lower bound $\Gamma_{\text{S'MoRE}}$ easily exceeds the upper bound Γ_{MoMOR} by orders of magnitude (even for just 2 layers; see Fig. 3). The reason is that for MoMOR, the $\binom{s_\ell}{i}$ terms are *summed* over F_ℓ , while for S'MoRE, F_ℓ becomes the *exponent* of $\binom{s_\ell}{f_\ell}$.

To prove Theorem 4.3, notice from Eq. (3) that the MoMOR output is generated by a flat summation of different-order residues. The number of distinct outputs that can be generated from a given input cannot exceed the number of distinct ways to select residues from the pools $\mathcal{R}_0, \dots, \mathcal{R}_{L-1}$. For the \mathcal{R}_{L-1} pool with size s_{L-1} , there are $\binom{s_{L-1}}{f_{L-1}}$ ways to pick f_{L-1} residues. For \mathcal{R}_{L-2} with $\ell \leq L-2$, there are $F_{\ell+1}$ parents, each picking f_ℓ children in the pool. Different parents can pick the same children. The number of distinct children selected by all parents ranges from f_ℓ to $\min\{F_\ell, s_\ell\}$, explaining the summation over i .

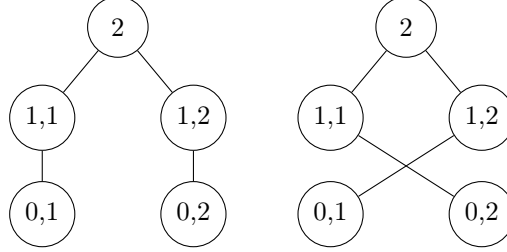


Figure 2 Example cases where the same set of experts are activated but are connected in two different ways. MoMOR will generate the same output for the two activation schemes, while S’MoRE can generate distinct outputs due to its higher structural flexibility.

From Theorem 4.4, S’MoRE increases the structural flexibility due to the non-linearity between layers. $\Gamma_{\text{S’MoRE}}$ counts the total number of *non-isomorphic* depth- L trees that can be formed by picking different experts in each layer. To derive $\Gamma_{\text{S’MoRE}}$, note that for each activated expert in $\mathcal{R}_{\ell+1}$, we have $\binom{s_\ell}{f_\ell}$ different ways to construct its children set. Each distinct children set always leads to a new non-isomorphic tree, regardless of how other parents in $\mathcal{R}_{\ell+1}$ pick their children. Thus, all activated parents belonging to $\mathcal{R}_{\ell+1}$ contribute to a $\binom{s_\ell}{f_\ell}^{F_{\ell+1}}$ factor of $\Gamma_{\text{S’MoRE}}$. Note that the exponent is simply $F_{\ell+1}$ rather than $\min\{F_{\ell+1}, s_{\ell+1}\}$. Fig. 2 illustrates the idea: we have $L = 2$ and node 2 is the final output node. In both cases, we activate the same set of 4 experts. The experts connect in two different ways. On the left, parent 1,1 connects to child 0,1, while on the right, parent 1,1 connects to 0,2. MoMOR will have the same output embedding for the two cases, since it only cares about the *set* of activated experts. S’MoRE can learn to generate different outputs corresponding to the two distinct interconnection patterns (i.e., the left and right trees are non-isomorphic).

To prove Theorem 4.4, the final question is whether the model defined by the layer propagation of Eq. (4) can perform the isomorphism test. We borrow known conclusions from the Graph Neural Network (GNN) literature. We can view Equation 4 as defining a variant of the Graph Isomorphism Network (GIN) (Xu et al., 2019). The L -layer propagation simulates the L -iteration Weisfeiler-Lehman (WL) test (Huang and Villar, 2021), where σ implemented as an MLP ensures an injective “color refinement” process in WL. It then follows that the L layer S’MoRE can distinguish non-isomorphic depth- L trees (given that in Equation 4, we can include an additional bias term unique to each expert / residual).

Although Theorem 4.4 sets σ as an MLP, in practice, we implement σ simply as non-linear activation (e.g., ReLU). It is easy to see that setting σ as “an MLP with a *single* hidden layer of dimension $d_{\ell+1}$ ” is equivalent to setting σ simply as an activation function, in the context of Eq. (4).

5 Experiments

5.1 Setup

Datasets. We conduct fine-tuning experiments on a diverse set of widely-used benchmarks, including ARC-c/e (Clark et al., 2018), Commonsense QA (Talmor et al., 2018), OpenBook QA (Mihaylov et al., 2018), and Winogrande (Sakaguchi et al., 2021). Specifically, ARC-c and ARC-e evaluate logical reasoning and world knowledge through challenging multiple-choice questions. Commonsense QA assesses a model’s grasp of everyday knowledge and implicit relationships. OpenBook QA requires multi-step reasoning over scientific facts, while Winogrande measures commonsense pronoun resolution. Accuracy is used as the evaluation metric for all above datasets.

Base models & baselines. We use the open-source pre-trained models, LLaMA-3.2-1B and LLaMA-3-8B (Dubey et al., 2024), as the base models, which covers different scales. We consider the fine-tuning task, where we insert low-rank adapters of different kinds: 1. LoRA (Hu et al., 2021) which does not have any routing mechanism; 2. mixture of LoRA experts (MixLoRA) (Li et al., 2024), which is a state-of-the-art parameter efficient MoE adapter using similar top- k routing as ours; 3. HydraLoRA (Tian et al., 2024), which is another state-of-the-art PEFT adapter implementing a MoE variant of LoRA by splitting LoRA’s single up-projection head \mathbf{B} into multiple matrices, and combining the multi-head outputs via weights generated by a dense gate; and 4. S’MoRE which can be seen as a multi-layer extension of LoRA and MixLoRA. To further evaluate the feasibility of applying S’MoRE to different model variants, we implement 3 variants of MixLoRA and S’MoRE by using different types of gates discussed in §4.3: two sparse gates (noisy top- k gate (Shazeer et al., 2017) and switch-transformer gate (Fedus et al., 2022b)), and one dense gate (the same as HydraLoRA (Tian et al., 2024)). For all models, we insert the adapters to the feed forward networks (FFN) of all transformer layers of the base models. Specifically, each FFN consists of an “up-projection” matrix, a “gate-projection” matrix and a “down-projection” matrix. We insert the adapter to each of the three matrices.

Training & evaluation methodology. For hyperparameter tuning, we train all models using the same number of epochs, learning rate schedule, gradient accumulation steps and machine type. To ensure a fair comparison, we set an equal budget for trainable adapter parameters and compare different model architecture within this constraint. For LoRA (Hu et al., 2021), we vary the rank r in $\{2^k \mid 0 \leq k \leq 10\}$, and set the α parameter as $2 \cdot r$ following standard practice. For MixLoRA (Li et al., 2024), we adjust the number of experts within $\{4, 8, 16\}$, keep the number of active experts within $\{1, 2, 4, 8\}$ ¹ (ensuring that it does not exceed half of the total experts), and the expert dimension within $\{2^k \mid 0 \leq k \leq 6\}$. For HydraLoRA (Tian et al., 2024), we vary the number of heads in $\{4, 8\}$, and the rank r in $\{2^k \mid 0 \leq k \leq 8\}$. For S’MoRE, in most experiments (except the “scaling-up” study in Table 4), we limit S’MoRE to two layers due to resource constraints. We vary the number of experts (s_0, s_1) within $\{(2, 2), (2, 4), (4, 4)\}$, the fanout (f_0, f_1) within $\{(1, 1), (2, 1), (2, 2)\}$ ², and the expert dimension (r_0, r_1) within $\{(2^k, 2^k) \mid 0 \leq k \leq 6\} \cup \{(2^k, 2^{k+1}) \mid 0 \leq k \leq 5\} \cup \{(2^k, 2^{k+2}) \mid 0 \leq k \leq 4\}$.

Software & hardware. We implement S’MoRE by adding a customized adapter to the Hugging Face PEFT library (Mangrulkar et al., 2022). All models are trained via the LLaMA-Factory (Zheng et al., 2024) SFT pipeline, ensuring a consistent execution environment. Similarly, all the evaluations are conducted through OpenCompass (Contributors, 2023), which is a unified evaluation framework providing a standard API for all considered benchmarks. All experiments are run on a single node with 4 NVIDIA A100 80GB GPUs.

5.2 Main Results

We summarize the main results on accuracy and number of trainable parameters in Table 2 and Table 3.

Baseline comparisons & ablations. We observe that for both LLaMA 3.2 1B and LLaMA 3 8B, S’MoRE consistently achieves significant accuracy improvements while being as parameter-efficient as the baselines – especially, compared with MixLoRA, S’MoRE **simultaneously achieves accuracy and parameter efficiency improvement** in most cases. In addition, the improvements of S’MoRE are observed across all 3 types of gates, implying that the S’MoRE design is *widely applicable* to different PEFT model variants. For LoRA, even through our hyperparameter search covers LoRA models with a high rank (up to $2^{10} = 1024$), simply increasing the rank does not effectively improves accuracy – the highest-accuracy LoRA models generally have low parameter counts. This shows the necessity of more advanced PEFT models such as the three MoE variants in Table 2 and Table 3. For HydraLoRA and MixLoRA, we set their experts’ rank and the total number of heads / experts to match those of S’MoRE (i.e., “ $4 = 2 + 2$ ” and “ $8 = 4 + 4$ ”). Under such comparable settings, the superior performance of S’MoRE clearly shows the benefits of breaking down a single layer of experts into an inter-connected 2-layer structure. These empirical findings validate our hypothesis that the greatly higher “structural flexibility” significantly enhances model capacity without incurring parameter overhead. Finally, due to resource constraints, we only evaluated the 16-expert MixLoRA for the noisy top- k

¹“Number of active experts” is only set for the sparse gates (“noisy top- k ” and “switch”). For dense gates, the number of active experts equals total number of experts.

²Same as above, the fanouts are only set for sparse gates. For dense gates, the fanout of layer ℓ equals the total number of experts in layer ℓ

Table 2 LLaMA 3.2-1B: Comparison of accuracy and trainable parameters (corresponding to the highest-accuracy model) for different adapter architectures. For HydraLoRA, MixLoRA and S’MoRE, the number of experts are enclosed by parentheses (e.g., “HydraLoRA (4)” means 4 heads for the up-projection \mathbf{B} matrices; “MixLoRA (4)” means a single-layer 4-expert architecture; “S’MoRE (4-4)” means a 2 layer structure each having 4 experts). We implemented 3 different gating architectures: “Dense” follows the HydraLoRA implementation, performing weighted sum of all experts’ outputs with the weights generated by the gate. “Noisy top- k ” and “Switch transformer” are two types of sparse gates widely used in SoTA LLM-MoE systems. Due to limited resources, we only conducted experiments for “MixLoRA (16)” and “S’MoRE (2-4)” for the noisy top- k gate.

Gate	PEFT model	ARC-c		ARC-e		Commonsense QA		OpenBook QA		Winogrande		Avg Acc	Avg Params
		Accuracy	Params (B)	Accuracy	Params (B)	Accuracy	Params (B)	Accuracy	Params (B)	Accuracy	Params (B)		
	LoRA	36.27	0.004	74.78	0.031	63.80	0.063	71.20	0.031	49.72	0.016	59.154	0.029
Dense	HydraLoRA (4)	35.93	0.006	73.54	0.023	66.34	0.023	71.60	0.023	50.75	0.012	59.632	0.0174
	HydraLoRA (8)	35.93	0.012	72.31	0.012	62.08	0.042	71.60	0.022	50.99	0.012	58.582	0.0200
	MixLoRA (4)	39.66	0.021	72.84	0.134	65.44	0.134	70.40	0.134	51.30	0.007	59.928	0.0860
	MixLoRA (8)	39.32	0.021	74.78	0.270	66.42	0.069	69.60	0.134	51.14	0.037	60.252	0.1062
	S’MoRE (2-2)	40.00	0.017	75.31	0.085	66.99	0.037	72.20	0.085	52.01	0.015	61.302	0.0478
	S’MoRE (4-4)	39.66	0.017	74.43	0.135	67.32	0.045	72.80	0.202	52.01	0.168	61.244	0.1134
Noisy top- k	MixLoRA (4)	39.32	0.037	71.96	0.069	64.70	0.134	70.00	0.134	51.46	0.069	59.488	0.0886
	MixLoRA (8)	37.97	0.069	72.84	0.270	65.03	0.134	70.80	0.270	51.46	0.069	59.620	0.1624
	MixLoRA (16)	37.29	0.134	73.90	0.270	64.13	0.270	71.00	0.270	51.54	0.270	59.572	0.2428
	S’MoRE (2-2)	39.66	0.029	73.19	0.135	64.95	0.135	70.00	0.102	51.54	0.029	59.868	0.0860
	S’MoRE (2-4)	38.64	0.037	74.43	0.202	65.68	0.135	69.60	0.053	51.93	0.037	60.056	0.0928
	S’MoRE (4-4)	39.66	0.037	74.96	0.135	66.26	0.102	71.40	0.135	52.17	0.273	60.890	0.1364
Switch transformer	MixLoRA (4)	38.98	0.021	73.37	0.134	66.42	0.069	72.00	0.134	51.22	0.009	60.398	0.0734
	MixLoRA (8)	39.32	0.021	73.72	0.069	65.85	0.134	71.80	0.134	51.30	0.021	60.398	0.0758
	S’MoRE (2-2)	39.66	0.037	74.78	0.135	66.75	0.069	71.40	0.102	52.25	0.045	60.968	0.0776
	S’MoRE (4-4)	40.34	0.021	74.78	0.168	67.16	0.202	72.40	0.085	52.09	0.021	61.354	0.0994

gate. In both Table 2 and Table 3, we observe that simply increasing the number of experts for a single-layer MoE model does not further improve accuracy. This implies that exploring the structural information can bring unique values to the current MoE research.

Structural flexibility. In §4.5, we theoretically demonstrate that S’MoRE is significantly more structurally flexible than existing MoMOR models. Based on Theorems 4.3 and 4.4, we calculate their structural flexibility under different number of layers L . In Fig. 3, we set $s_\ell = 4$ and $f_\ell = 2$ for all layers ℓ . Clearly, 1. the structural flexibility of S’MoRE is substantially higher than that of MoMOR, even for shallow models of 2 layers. 2. the structural flexibility of S’MoRE grows exponentially more faster than that of MoMOR when increasing the number of layers L .

5.3 Scaling up

We further evaluate if scaling up the number of layers of S’MoRE can further improve accuracy. We follow a simple hyperparameter tuning strategy: for all the 2-layer S’MoRE under consideration, we add a 3rd layer with identical configuration (w.r.t. number of experts s , fanout f , expert dimension r , etc.) as the 2nd layer. In other words, the sizes of the design spaces for the 3-layer and 2-layer S’MoRE are equal.

Table 4 summarizes the comparison for different 2-layer and 3-layer architectures. Adding an additional layer does further improve accuracy significantly in most cases. In addition, such accuracy improvements do not necessarily come at the cost of more parameters. For example, for Winogrande, the “2-2-2” structure improves the accuracy of “2-2” by 0.87 while saving 27% parameters. Notably, the superior performance of the 3-layer models are achieved by simply applying the “naive” hyperparameter searching strategy for the 3-layer models (see above). With more comprehensive tuning on the 3rd layer, we may further boost the 3-layer model performance.

5.4 Analysis on router

In Fig. 4, we visualize the router computation cost (Eq. (9)) relative to that of the experts’ layer propagation (Eq. (4)), corresponding to the best-performing models in Table 2. The x -axis denotes the different S’MoRE structures. The costs are measured by the total number of arithmetic operations performed by the routers

Table 3 LLaMA 3-8B: Comparison of accuracy and trainable parameters (corresponding to the highest-accuracy model) for different adapter architecture. We follow the same setup as Table 2.

Gate	PEFT model	ARC-c		ARC-e		Commonsense QA		OpenBook QA		Winogrande		Avg Acc	Avg Params
		Accuracy	Params (B)	Accuracy	Params (B)	Accuracy	Params (B)	Accuracy	Params (B)	Accuracy	Params (B)		
Dense	LoRA	81.69	0.028	91.36	0.028	81.00	0.028	87.00	0.028	81.77	0.028	84.564	0.028
	HydraLoRA (4)	83.39	0.082	91.53	0.160	81.82	0.013	88.20	0.082	83.82	0.160	85.752	0.0994
	HydraLoRA (8)	81.69	0.152	91.53	0.015	81.49	0.024	86.60	0.042	84.14	0.297	85.090	0.1060
	MixLoRA (4)	81.69	0.026	92.24	0.247	81.24	0.033	89.40	0.478	84.06	0.247	85.726	0.2062
	MixLoRA (8)	82.37	0.132	91.71	0.247	81.00	0.033	88.60	0.075	85.40	0.478	85.816	0.1930
	S'MoRE (2-2)	82.37	0.090	92.24	0.190	81.90	0.037	89.40	0.054	88.24	0.480	86.830	0.1702
Noisy top-k	S'MoRE (4-4)	82.71	0.190	91.89	0.247	81.90	0.033	90.00	0.076	85.48	0.247	86.396	0.1586
	MixLoRA (4)	82.37	0.075	91.53	0.478	80.75	0.075	87.80	0.075	82.00	0.478	84.890	0.2362
	MixLoRA (8)	83.39	0.950	91.53	0.950	80.67	0.075	88.40	0.247	83.19	0.478	85.436	0.5400
	MixLoRA (16)	82.03	0.951	91.36	0.478	80.84	0.132	88.20	0.478	82.08	0.478	84.902	0.5034
	S'MoRE (2-2)	82.37	0.305	91.36	0.090	81.82	0.104	88.20	0.047	83.27	0.190	85.404	0.1472
	S'MoRE (2-4)	83.05	0.714	91.36	0.090	81.57	0.040	88.80	0.147	83.90	0.537	85.736	0.3056
Switch transformer	S'MoRE (4-4)	82.37	0.104	91.71	0.305	82.06	0.047	90.00	0.480	85.48	0.714	86.324	0.3300
	MixLoRA (4)	82.37	0.132	92.95	0.478	81.08	0.047	88.80	0.478	84.53	0.247	85.946	0.2764
	MixLoRA (8)	82.03	0.047	91.71	0.132	81.24	0.047	88.60	0.247	85.95	0.950	85.906	0.2846
	S'MoRE (2-2)	83.05	0.133	92.24	0.061	81.82	0.029	89.80	0.076	86.42	0.247	86.666	0.1092
	S'MoRE (4-4)	83.39	0.076	92.42	0.305	82.15	0.047	89.80	0.305	85.87	0.305	86.726	0.2076

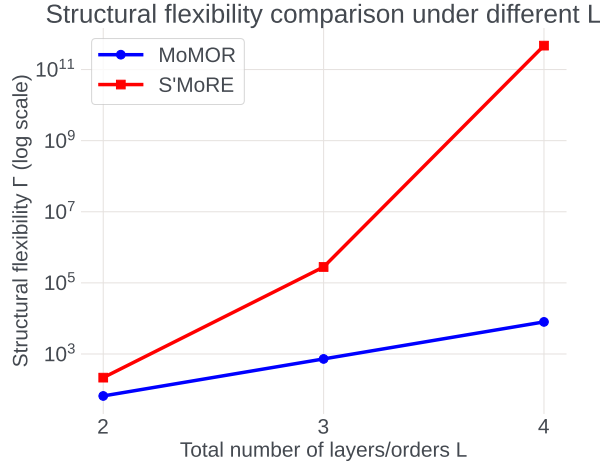


Figure 3 Theoretical structural flexibility under different number of layers (for S'MoRE) or orders (for MoMoRE)

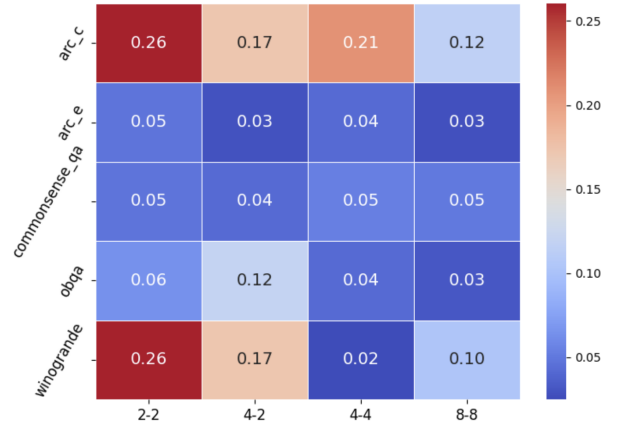


Figure 4 Cost of router relative to expert propagation, measured by number of arithmetic operations

or the experts. In general, when the residual rank r_ℓ is lower, the cost of routing becomes *relatively* higher (since the router operation is independent of the ranks). However, in all cases, the routing cost is insignificant compared to the cost of expert propagation (at most 26%). This is consistent with our theoretical complexity analysis in §4.4.

6 Conclusion

We introduced S'MoRE, a novel Structural Mixture of Residual Experts framework that unifies the efficiency of low-rank adaptation (LoRA) with the flexibility of Mixture-of-Experts (MoE), and further boosts the model capacity of MoE by exploiting experts' inherent structure. By leveraging a hierarchical residual decomposition and tree-based routing, S'MoRE effectively increases the number of experts without significant computational overhead. Our theoretical analysis demonstrates that S'MoRE generalizes and surpasses existing LoRA-MoE hybrids under a novel structural flexibility metric, while empirical results confirm its state-of-the-art fine-tuning performance across multiple reasoning and domain-specific benchmarks. Specifically, compared to standard LoRA and MoE models, S'MoRE achieves superior accuracy (+2.1%) while reducing the number of trainable parameters. Our ablation studies highlight the necessity of hierarchical routing and multi-order residuals, showing that deeper expert hierarchies enhance performance without incurring excessive computation costs.

Table 4 S'MoRE on LLaMA 3.2-1B: Scaling up the number of layers helps further improve accuracy with high parameter efficiency. We follow a simple hyperparameter tuning strategy for the 3-layer models: for all the 2-layer S'MoRE within the design space, we add a 3rd layer with identical configuration (number of experts, fanout, expert dimension, etc.) as the 2nd layer. With a more thorough tuning on the 3rd layer parameters, the 3-layer model performance may improve further.

Layer sizes	ARC-c		ARC-e		Commonsense QA		OpenBook QA		Winogrande	
	Accuracy	Params (B)	Accuracy	Params (B)	Accuracy	Params (B)	Accuracy	Params (B)	Accuracy	Params (B)
2-2	40.00	0.017	75.31	0.085	66.99	0.037	72.20	0.085	52.01	0.015
2-2-2	39.32	0.017	74.25	0.102	67.40	0.053	72.60	0.205	52.88	0.011
4-4	39.66	0.017	74.43	0.135	67.32	0.045	72.80	0.202	52.01	0.168
4-4-4	40.34	0.029	73.90	0.205	67.32	0.053	73.60	0.202	52.09	0.013

Additionally, our structural flexibility analysis provides insight into how multi-layer expert selection improves adaptive fine-tuning capacity beyond conventional MoE architectures.

References

- Josh Achiam, Steven Adler, Sandhini Agarwal, Lama Ahmad, Ilge Akkaya, Florencia Leoni Aleman, Diogo Almeida, Janko Altenschmidt, Sam Altman, Shyamal Anadkat, et al. Gpt-4 technical report. *arXiv preprint arXiv:2303.08774*, 2023.
- AF Agarap. Deep learning using rectified linear units (relu). *arXiv preprint arXiv:1803.08375*, 2018.
- Joshua Ainslie, Tao Lei, Michiel de Jong, Santiago Ontañón, Siddhartha Brahma, Yury Zemlyanskiy, David Uthus, Mandy Guo, James Lee-Thorp, Yi Tay, et al. Colt5: Faster long-range transformers with conditional computation. *arXiv preprint arXiv:2303.09752*, 2023.
- Anthropic. The claude 3 model family: Opus, sonnet, haiku. 2024. <https://api.semanticscholar.org/CorpusID:268232499>.
- Weilin Cai, Juyong Jiang, Fan Wang, Jing Tang, Sunghun Kim, and Jiayi Huang. A survey on mixture of experts. *arXiv preprint arXiv:2407.06204*, 2024.
- Zhaorun Chen, Yichao Du, Zichen Wen, Yiyang Zhou, Chenhang Cui, Zhenzhen Weng, Haoqin Tu, Chaoqi Wang, Zhengwei Tong, Qinglan Huang, et al. Mj-bench: Is your multimodal reward model really a good judge for text-to-image generation? *arXiv preprint arXiv:2407.04842*, 2024.
- Peter Clark, Isaac Cowhey, Oren Etzioni, Tushar Khot, Ashish Sabharwal, Carissa Schoenick, and Oyvind Tafjord. Think you have solved question answering? try arc, the ai2 reasoning challenge. *arXiv preprint arXiv:1803.05457*, 2018.
- OpenCompass Contributors. Opencompass: A universal evaluation platform for foundation models. <https://github.com/open-compass/opencompass>, 2023.
- Damai Dai, Chengqi Deng, Chenggang Zhao, R. X. Xu, Huazuo Gao, Deli Chen, Jiashi Li, Wangding Zeng, Xingkai Yu, Y. Wu, Zhenda Xie, Y. K. Li, Panpan Huang, Fuli Luo, Chong Ruan, Zhifang Sui, and Wenfeng Liang. Deepseekmoe: Towards ultimate expert specialization in mixture-of-experts language models, 2024. <https://arxiv.org/abs/2401.06066>.
- DeepSeek-AI. Deepseek-v3 technical report, 2024. <https://arxiv.org/abs/2412.19437>.
- Shihan Dou, Enyu Zhou, Yan Liu, Songyang Gao, Wei Shen, Limao Xiong, Yuhao Zhou, Xiao Wang, Zhiheng Xi, Xiaoran Fan, Shiliang Pu, Jiang Zhu, Rui Zheng, Tao Gui, Qi Zhang, and Xuanjing Huang. LoRAMoE: Alleviating world knowledge forgetting in large language models via MoE-style plugin. In Lun-Wei Ku, Andre Martins, and Vivek Srikumar, editors, *Proceedings of the 62nd Annual Meeting of the Association for Computational Linguistics (Volume 1: Long Papers)*, pages 1932–1945, Bangkok, Thailand, August 2024. Association for Computational Linguistics. doi: 10.18653/v1/2024.acl-long.106. <https://aclanthology.org/2024.acl-long.106>.
- Abhimanyu Dubey, Abhinav Jauhri, Abhinav Pandey, Abhishek Kadian, Ahmad Al-Dahle, Aiesha Letman, Akhil Mathur, Alan Schelten, Amy Yang, Angela Fan, et al. The llama 3 herd of models. *arXiv preprint arXiv:2407.21783*, 2024.
- William Fedus, Jeff Dean, and Barret Zoph. A review of sparse expert models in deep learning, 2022a. <https://arxiv.org/abs/2209.01667>.
- William Fedus, Barret Zoph, and Noam Shazeer. Switch transformers: Scaling to trillion parameter models with simple and efficient sparsity. *Journal of Machine Learning Research*, 23(120):1–39, 2022b.
- Muhammad Usman Hadi, Rizwan Qureshi, Abbas Shah, Muhammad Irfan, Anas Zafar, Muhammad Bilal Shaikh, Naveed Akhtar, Jia Wu, Seyedali Mirjalili, et al. A survey on large language models: Applications, challenges, limitations, and practical usage. *Authorea Preprints*, 2023.
- Xu Owen He. Mixture of a million experts, 2024. <https://arxiv.org/abs/2407.04153>.
- Edward J Hu, Yelong Shen, Phillip Wallis, Zeyuan Allen-Zhu, Yuanzhi Li, Shean Wang, Lu Wang, and Weizhu Chen. Lora: Low-rank adaptation of large language models. *arXiv preprint arXiv:2106.09685*, 2021.
- Ningyuan Teresa Huang and Soledad Villar. A short tutorial on the weisfeiler-lehman test and its variants. In *ICASSP 2021 - 2021 IEEE International Conference on Acoustics, Speech and Signal Processing (ICASSP)*, page 8533–8537. IEEE, June 2021. doi: 10.1109/icassp39728.2021.9413523. <http://dx.doi.org/10.1109/ICASSP39728.2021.9413523>.

- Dawid Jan Kopiczko, Tijmen Blankevoort, and Yuki M Asano. VeRA: Vector-based random matrix adaptation. In *The Twelfth International Conference on Learning Representations*, 2024. <https://openreview.net/forum?id=NjNfLdxr3A>.
- Dmitry Lepikhin, Hyoungho Lee, Yuanzhong Xu, Dehao Chen, Orhan Firat, Yanping Huang, Maxim Krikun, Noam Shazeer, and Zhifeng Chen. Gshard: Scaling giant models with conditional computation and automatic sharding. *arXiv preprint arXiv:2006.16668*, 2020.
- Dengchun Li, Yingzi Ma, Naizheng Wang, Zhiyuan Cheng, Lei Duan, Jie Zuo, Cal Yang, and Mingjie Tang. Mixlora: Enhancing large language models fine-tuning with lora based mixture of experts. *arXiv preprint arXiv:2404.15159*, 2024.
- Chen Ling, Xujiang Zhao, Jiaying Lu, Chengyuan Deng, Can Zheng, Junxiang Wang, Tanmoy Chowdhury, Yun Li, Hejie Cui, Xuchao Zhang, et al. Domain specialization as the key to make large language models disruptive: A comprehensive survey. *arXiv preprint arXiv:2305.18703*, 2023.
- Aixin Liu, Bei Feng, Bing Xue, Bingxuan Wang, Bochao Wu, Chengda Lu, Chenggang Zhao, Chengqi Deng, Chenyu Zhang, Chong Ruan, et al. Deepseek-v3 technical report. *arXiv preprint arXiv:2412.19437*, 2024a.
- Haokun Liu, Derek Tam, Mohammed Muqeeth, Jay Mohta, Tenghao Huang, Mohit Bansal, and Colin Raffel. Few-shot parameter-efficient fine-tuning is better and cheaper than in-context learning, 2022. <https://arxiv.org/abs/2205.05638>.
- Shih-Yang Liu, Chien-Yi Wang, Hongxu Yin, Pavlo Molchanov, Yu-Chiang Frank Wang, Kwang-Ting Cheng, and Min-Hung Chen. DoRA: Weight-decomposed low-rank adaptation. In Ruslan Salakhutdinov, Zico Kolter, Katherine Heller, Adrian Weller, Nuria Oliver, Jonathan Scarlett, and Felix Berkenkamp, editors, *Proceedings of the 41st International Conference on Machine Learning*, volume 235 of *Proceedings of Machine Learning Research*, pages 32100–32121. PMLR, 21–27 Jul 2024b. <https://proceedings.mlr.press/v235/liu24bn.html>.
- Yuqing Liu, Yu Wang, Lichao Sun, and Philip S Yu. Rec-gpt4v: Multimodal recommendation with large vision-language models. *arXiv preprint arXiv:2402.08670*, 2024c.
- Jan Ludziejewski, Jakub Krajewski, Kamil Adamczewski, Maciej Pióro, Michał Krutul, Szymon Antoniak, Kamil Ciebiera, Krystian Król, Tomasz Odrzygóźdź, Piotr Sankowski, Marek Cygan, and Sebastian Jaszczur. Scaling laws for fine-grained mixture of experts. In Ruslan Salakhutdinov, Zico Kolter, Katherine Heller, Adrian Weller, Nuria Oliver, Jonathan Scarlett, and Felix Berkenkamp, editors, *Proceedings of the 41st International Conference on Machine Learning*, volume 235 of *Proceedings of Machine Learning Research*, pages 33270–33288. PMLR, 21–27 Jul 2024. <https://proceedings.mlr.press/v235/ludziejewski24a.html>.
- Sourab Mangrulkar, Sylvain Gugger, Lysandre Debut, Younes Belkada, Sayak Paul, and Benjamin Bossan. Peft: State-of-the-art parameter-efficient fine-tuning methods. <https://github.com/huggingface/peft>, 2022.
- Yuren Mao, Yuhang Ge, Yijiang Fan, Wenyi Xu, Yu Mi, Zhonghao Hu, and Yunjun Gao. A survey on lora of large language models. *Frontiers of Computer Science*, 19(7):197605, 2025.
- Todor Mihaylov, Peter Clark, Tushar Khot, and Ashish Sabharwal. Can a suit of armor conduct electricity? a new dataset for open book question answering. In *EMNLP*, 2018.
- Joan Puigcerver, Carlos Riquelme Ruiz, Basil Mustafa, and Neil Houlsby. From sparse to soft mixtures of experts. In *The Twelfth International Conference on Learning Representations*, 2024. <https://openreview.net/forum?id=jxpsAj7ltE>.
- Samyam Rajbhandari, Conglong Li, Zhewei Yao, Minjia Zhang, Reza Yazdani Aminabadi, Ammar Ahmad Awan, Jeff Rasley, and Yuxiong He. DeepSpeed-MoE: Advancing mixture-of-experts inference and training to power next-generation AI scale. In Kamalika Chaudhuri, Stefanie Jegelka, Le Song, Csaba Szepesvari, Gang Niu, and Sivan Sabato, editors, *Proceedings of the 39th International Conference on Machine Learning*, volume 162 of *Proceedings of Machine Learning Research*, pages 18332–18346. PMLR, 17–23 Jul 2022. <https://proceedings.mlr.press/v162/rajbhandari22a.html>.
- David Raposo, Sam Ritter, Blake Richards, Timothy Lillicrap, Peter Conway Humphreys, and Adam Santoro. Mixture-of-depths: Dynamically allocating compute in transformer-based language models, 2024. <https://arxiv.org/abs/2404.02258>.
- Keisuke Sakaguchi, Ronan Le Bras, Chandra Bhagavatula, and Yejin Choi. Winogrande: An adversarial winograd schema challenge at scale. *Communications of the ACM*, 64(9):99–106, 2021.

- Noam Shazeer, Azalia Mirhoseini*, Krzysztof Maziarczyk*, Andy Davis, Quoc Le, Geoffrey Hinton, and Jeff Dean. Outrageously large neural networks: The sparsely-gated mixture-of-experts layer. In *International Conference on Learning Representations*, 2017. <https://openreview.net/forum?id=B1ckMDq1g>.
- Alon Talmor, Jonathan Herzig, Nicholas Lourie, and Jonathan Berant. Commonsenseqa: A question answering challenge targeting commonsense knowledge. *arXiv preprint arXiv:1811.00937*, 2018.
- Amara Tariq, Man Luo, Aisha Urooj, Avisha Das, Jiwoong Jeong, Shubham Trivedi, Bhavik Patel, and Imon Banerjee. Domain-specific llm development and evaluation—a case-study for prostate cancer. *medRxiv*, pages 2024–03, 2024.
- Gemini Team, Petko Georgiev, Ving Ian Lei, Ryan Burnell, Libin Bai, Anmol Gulati, Garrett Tanzer, Damien Vincent, Zhufeng Pan, Shibo Wang, et al. Gemini 1.5: Unlocking multimodal understanding across millions of tokens of context. *arXiv preprint arXiv:2403.05530*, 2024.
- Chunlin Tian, Zhan Shi, Zhijiang Guo, Li Li, and Chengzhong Xu. Hydralora: An asymmetric lora architecture for efficient fine-tuning. In *Advances in Neural Information Processing Systems (NeurIPS)*, 2024.
- Chaoqi Wang, Zhuokai Zhao, Chen Zhu, Karthik Abinav Sankararaman, Michal Valko, Xuefei Cao, Zhaorun Chen, Madian Khabsa, Yuxin Chen, Hao Ma, et al. Preference optimization with multi-sample comparisons. *arXiv preprint arXiv:2410.12138*, 2024a.
- Chaoqi Wang, Zhuokai Zhao, Yibo Jiang, Zhaorun Chen, Chen Zhu, Yuxin Chen, Jiayi Liu, Lizhu Zhang, Xiangjun Fan, Hao Ma, et al. Beyond reward hacking: Causal rewards for large language model alignment. *arXiv preprint arXiv:2501.09620*, 2025.
- Luping Wang, Sheng Chen, Linnan Jiang, Shu Pan, Runze Cai, Sen Yang, and Fei Yang. Parameter-efficient fine-tuning in large models: A survey of methodologies. *arXiv preprint arXiv:2410.19878*, 2024b.
- Xun Wu, Shaohan Huang, and Furu Wei. Mixture of loRA experts. In *The Twelfth International Conference on Learning Representations*, 2024. <https://openreview.net/forum?id=uWvKBCYh4S>.
- Keyulu Xu, Weihua Hu, Jure Leskovec, and Stefanie Jegelka. How powerful are graph neural networks? In *International Conference on Learning Representations*, 2019. <https://openreview.net/forum?id=ryGs6iA5Km>.
- Shengbin Yue, Shujun Liu, Yuxuan Zhou, Chenchen Shen, Siyuan Wang, Yao Xiao, Bingxuan Li, Yun Song, Xiaoyu Shen, Wei Chen, et al. Lawllm: Intelligent legal system with legal reasoning and verifiable retrieval. In *International Conference on Database Systems for Advanced Applications*, pages 304–321. Springer, 2024.
- Ted Zadori, Ahmet Üstün, Arash Ahmadian, Beyza Ermis, Acyr Locatelli, and Sara Hooker. Pushing mixture of experts to the limit: Extremely parameter efficient moe for instruction tuning. In *The Twelfth International Conference on Learning Representations*, 2024. <https://openreview.net/forum?id=EvDeiLv7qc>.
- Hanqing Zeng, Hanjia Lyu, Diyi Hu, Yinglong Xia, and Jiebo Luo. Mixture of weak and strong experts on graphs. In *The Twelfth International Conference on Learning Representations*, 2024. <https://openreview.net/forum?id=wYvuY60SdD>.
- Shengyu Zhang, Linfeng Dong, Xiaoya Li, Sen Zhang, Xiaofei Sun, Shuhe Wang, Jiwei Li, Runyi Hu, Tianwei Zhang, Fei Wu, et al. Instruction tuning for large language models: A survey. *arXiv preprint arXiv:2308.10792*, 2023.
- Yaowei Zheng, Richong Zhang, Junhao Zhang, Yanhan Ye, Zheyang Luo, Zhangchi Feng, and Yongqiang Ma. Llmfactory: Unified efficient fine-tuning of 100+ language models. In *Proceedings of the 62nd Annual Meeting of the Association for Computational Linguistics (Volume 3: System Demonstrations)*, Bangkok, Thailand, 2024. Association for Computational Linguistics. <http://arxiv.org/abs/2403.13372>.